

Evaluation of mechanical property and bioactivity of nano-bioglass 45S5 scaffold coated with poly-3-hydroxybutyrate

Mahbobeh Montazeri · Saeed Karbasi ·
Mohammad Reza Foughi · Ahmad Monshi ·
Reza Ebrahimi-Kahrizsangi

Received: 11 May 2014 / Accepted: 12 September 2014 / Published online: 29 January 2015
© Springer Science+Business Media New York 2015

Abstract One of the major challenges facing researchers of tissue engineering is scaffold design with desirable physical and mechanical properties for growth and proliferation of cells and tissue formation. In this research, firstly, nano-bioglass powder with grain sizes of 55–56 nm was prepared by melting method of industrial raw materials at 1,400 °C. Then the porous ceramic scaffold of bioglass with 30, 40 and 50 wt% was prepared by using the polyurethane sponge replication method. The scaffolds were coated with poly-3-hydroxybutyrate (P3HB) for 30 s and 1 min in order to increase the scaffold's mechanical properties. XRD, XRF, SEM, FE-SEM and FT-IR were used for phase and component studies, morphology, particle size and determination of functional groups, respectively. XRD and XRF results showed that the type of the produced bioglass was 45S5. The results of XRD and FT-IR showed that the best temperature to produce bioglass scaffold was 600 °C, in which $\text{Na}_2\text{Ca}_2\text{Si}_3\text{O}_9$ crystal is obtained. By coating the scaffolds with P3HB, a composite

scaffold with optimal porosity of 80–87 % in 200–600 μm and compression strength of 0.1–0.53 MPa was obtained. According to the results of compressive strength and porosity tests, the best kind of scaffold was produced with 30 wt% of bioglass immersed for 1 min in P3HB. To evaluate the bioactivity of the scaffold, the SBF solution was used. The selected scaffold (30 wt% bioglass/6 wt% P3HB) was maintained for up to 4 weeks in this solution at an incubation temperature of 37 °C. The XRD, SEM EDXA and AAS tests were indicative of hydroxyapatite formation on the surface of bioactive scaffold. This scaffold has some potential to use in bone tissue engineering.

1 Introduction

Every year, countless people suffer tissue injuries, such as bone injuries, due to different factors caused by accidents and automobile accidents, birth defects or loss of bone because of disease and various cancers [1]. The use of biodegradable materials is possible for tissue engineering, especially for bone tissue engineering, allowing reconstruction of damaged tissues. In some cases it is possible to replace lost or damaged tissue [2]. Tissue engineering is the science of design and production of new tissues to repair damaged organs and lost parts [3]. Among body tissues, bones have a high potential for regeneration. In fractures and large defects, efforts made by the body are not sufficient and bone grafting should be performed [4]. Among all the bioactive materials, the best bioactivity behavior belongs to bioactive glasses that contain a group of compounds that connect tissues in a short time [5]. In addition, these bioactive glasses prevent the formation of root tissue at implant–bone interface and encourage formation of a strong chemical bond between the implant and

M. Montazeri
Department of Materials Engineering, Young Researchers and
Elite Club, Najafabad Branch, Islamic Azad University,
Najafabad, Isfahan, Iran

S. Karbasi (✉)
Medical Physics and Biomedical Engineering Group, School of
Medicine, Isfahan University of Medical Sciences, Isfahan, Iran
e-mail: karbasi@med.mui.ac.ir

M. R. Foughi
Dental Materials Research Center, School of Dentistry, Isfahan
University of Medical Sciences, Isfahan, Iran

A. Monshi · R. Ebrahimi-Kahrizsangi
Department of Materials Engineering, Najafabad Branch,
Islamic Azad University, Isfahan, Iran

bone tissue [6]. Bioactive glasses are produced by melting and sol–gel methods [7]. There are various methods to produce porous scaffolds with suitable porosity and suitable physical conditions. The reproducible method of polymer is a suitable technique for manufacturing scaffolds with an adjustable porosity; polyurethane foam can be used for this purpose [8]. Since ceramic scaffolds have low strength and fracture resistance and cannot be used alone to reconstruct the osseous tissue, the polymer can be used as a reinforcing phase to enhance the mechanical properties of ceramic scaffolds. Many other components of biodegradable polymers and bioactive ceramics have been utilized as biocompatible scaffolds in tissue engineering. Poly-hydroxyalkanoate (PHA) is a biodegradable polymer used in tissue regeneration, drug delivery and patches, either alone or in composite form [9]. One member of the PHA family is poly-3-hydroxybutyrate (P3HB), which has a longer degradation time than poly α -hydroxy acids (for example, PLA and PLGA) and can be produced by various organisms [10]. P3HB is biocompatible with many different types of cells. P3HB does not degrade into acidic by-products, while degraded PLGA acidifies the immediate environment around the cell [11]. P3HB also has piezoelectric properties, which can play a critical role in stimulating bone growth and regeneration [12]. Bretcanu et al. [13] used bacteria-derived P3HB to infiltrate 45S5 bioglass scaffolds intended for use in cancellous bone substitution after traumatic incidents. Foroughi et al. [14] have covered composite scaffolds of hydroxyapatite nano-crystal with P3HB, with a porosity of 80–90 %, compressive strength and modulus, 1.51 and 22.73 MPa, respectively. Given that research study carried out by Hajiali et al. and Saadat et al. [7, 15], showed good results for P3HB based composite scaffolds with nano particles of HA and bioglass. But by comparing of these studies, it is so clear that one of the best achievements for bone tissue engineering is to cover ceramic scaffolds with polymer layers.

To the best of our knowledge, this is the first report on the formation of scaffolds from nano-bioglass (NBG) coated with P3HB. NBG powder was prepared using a melting industrial method, and porous scaffolds were constructed using a polymer replication method. In order to enhance mechanical properties, scaffolds were dip-coated with P3HB.

2 Materials and methods

2.1 Preparation of bioactive glass ceramic powder

Raw materials, including silica, sodium carbonate, calcium carbonate and phosphorus oxides, were mixed together. In order to engage the particles of SiO₂, compounds were

ball-milled for 30 min and to produce a greater amount of bioglass powder, the compounds were compressed after being ball-milled within the steel frame under pressure. Then the compressed pieces were melted in an alumina crucible at a temperature of 1,400 °C and the resulting melt was drained fast on a copper plate. The resultant glass was again ball-milled for 10 h. Then the produced powder was subjected to XRD, FE-SEM, XRF and FTIR tests (Table 1).

2.2 Fabrication of ceramic slurry

Preparation of slurry stabilized with proper additives is critical to scaffold formation; a variety of additives with a range of biological properties have been studied [16]. In this research, NBG powder with a grain size of 55–65 nm was utilized as the scaffold matrix. NBG (30, 40 and 50 wt%) was slowly dissolved in double-distilled water to prevent agglomeration. The slurry was stirred at 300 rpm for 90 min to produce a homogeneous solution. To maximize mechanical strength, large amounts of solid material should precipitate from the homogenized solution onto the polyurethane sponge. Ammonium poly-methacrylate (DARVAN[®]C–N, R.T. Vanderbilt Company, Norwalk, USA) was used to increase the weight percentage of solid substance to more than 2 wt%. Carboxymethyl cellulose (CMC, Hangzhou Hongbo Chemical Co. Ltd, China) powder (1.5 wt%) was gradually and slowly added to the solution in order to increase slurry flow. The solution was stirred at 60 °C until it was fully homogeneous.

2.3 Preparation of porous NBG scaffold

A commercial polyurethane sponge (MEAY Co., Ltd. China; average pore size of 300–700 μ m) was used in this

Table 1 Chemical analysis of nano-bioglass powder

Compound	Concentration (%W/W)
SiO ₂	41.04
CaO	29.25
Na ₂ O	23.26
Al ₂ O ₃	2.68
P ₂ O ₅	2.53
MgO	0.675
Fe ₂ O ₃	0.169
Cl	0.072
SO ₃	0.030
CuO	0.015
SrO	0.010
LOI*	0.59
Total	99.91

* Loss on ignition (1,400 °C, 90 min)

study. The sponge was immersed in ceramic slurry and squeezed twice. The resultant porous body was dried for 24 h in air.

Subsequently, the scaffolds were placed in a heat treatment furnace. The NBG scaffold was formed in four stages: (1) treatment at 400 °C, with a heating rate of 2 °C/min for 1 h, to completely burn the sponge; (2) an increase in temperature from 400 to 600 °C at a rate of 2 °C/min; (3) treatment at two different temperature; 600 and 1,000 °C for 5 h to sinter the ceramic scaffold; and (4) cooling to room temperature at a cooling rate of 5 °C/min. The cooled samples were removed from the furnace, measured and then placed in desiccators. Figure 1 shows the fabrication process of NBG porous scaffold and Fig. 2 shows the sponge and scaffold formed at 600 °C.

2.4 Bioglass scaffold coated with P3HB

In this study, 0.6 g of P3HB powder (Sigma-Aldrich, St Louis, MO, USA) was dissolved and heated in 10 mL of chloroform (Sigma-Aldrich, USA) for 6 h in an oil bath with a reflux condenser at 60 °C to produce the polymer solution for coating the ceramic scaffold. Next, NBG scaffolds were immersed in the polymer solution for 30 s and 1 min. To achieve a uniformly coated surface and remove excess polymer solution, the samples were wrapped in aluminum foil and centrifuged at 500 rpm for 30 s. Finally, the samples were placed in a vacuum oven at room temperature for 24 h.

Fig. 1 Flow chart of the polymer replication method used for the fabrication of NBG scaffolds

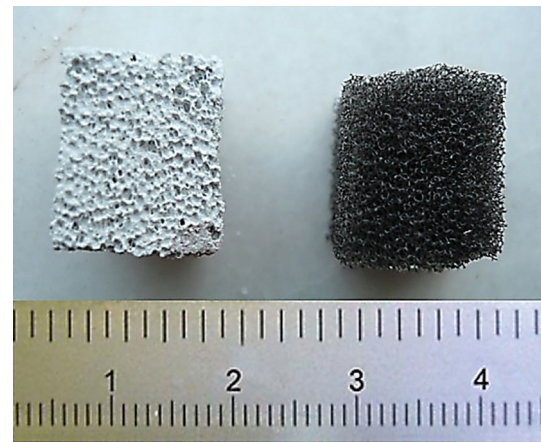
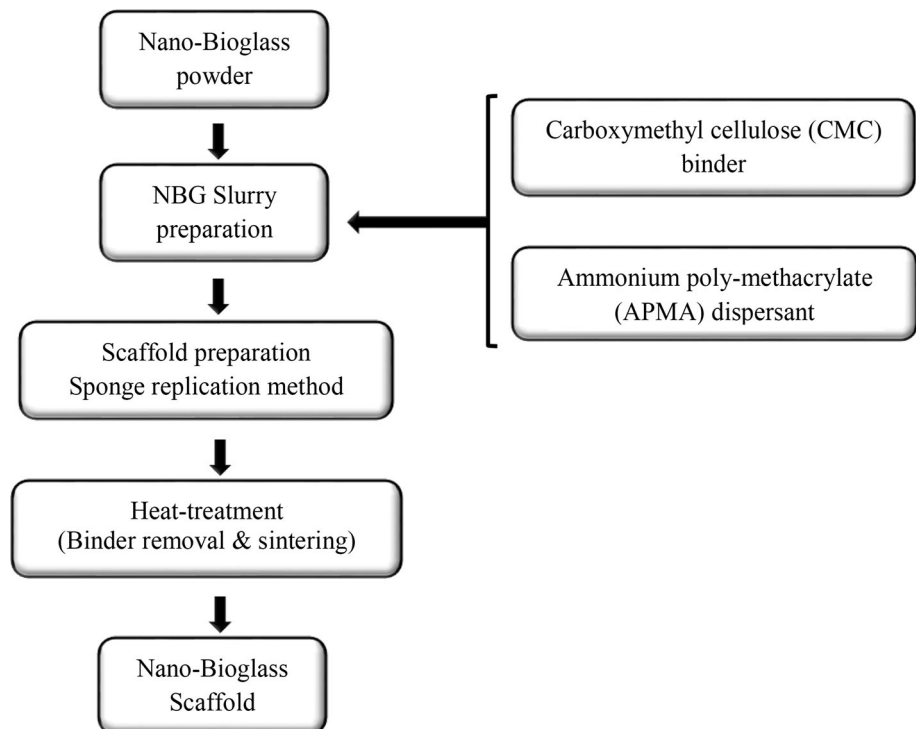


Fig. 2 Ceramic porous scaffold after heat treatment in 600 °C

2.5 Physical characterization

2.5.1 X-ray diffraction analysis

X-ray diffraction methods (XRD, Philips X'Pert) were applied to gain information about the structural changes and phases of NBG and scaffolds. Cu K α -ray was used for analysis. The scan rate was set to 1°/min; the imposed voltage and current were 40 kV and 30 mA, respectively, and the diffraction angle (2 θ) varied from 10° to 90° at a rate of 0.4°/min.

2.5.2 XRF analysis

XRF analysis is used for chemical analysis and for determination of chemical composition of bioglass. Elements with low atomic weight (H_2 , He and Li) cannot be identified with XRF; however, all the other elements can be identified.

2.5.3 FT-IR spectroscopy

IR was used to characterize NBG and scaffolds after sintering. A 2-mg dried sample was carefully mixed with 300 mg of dry KBr and compressed into a pellet using a macro KBr die kit. The solid pellet was placed in a magnetic holder. The system was purged with dry air for 1 h to remove water vapor from the sample compartment. Fourier transform infrared spectroscopy (FT-IR: 6300, JASCO, Japan) was used for studying functional groups and specifically, the degree of 2-hydroxylation of NBG. Spectral analyses were performed using standard Nicolet and Microrcal Origin software. FT-IR spectra were taken both as-received and sintered NBG and scaffolds.

2.5.4 Field emission scanning electron microscopy (FE-SEM)

Field emission scanning electron microscopy (FE-SEM, Philips XL-30, Netherlands) was used to study the NBG nano-crystals. Samples were coated with gold under an argon atmosphere.

2.5.5 Thermal gravity analysis (TGA)

Thermal gravity analysis (TGA) measures thermal stability and compounding materials. In this research, a TGA device (TG/DTA, TGA 401, Sanatara Co.) was used to record the weight percentage decrease of the polyurethane sponge versus temperature. The sample was heated at a rate of 1 °C/min, up to 600 °C, under nitrogen flow.

2.5.6 Porosity and density measurements

Liquid displacement was used to calculate the porosity and density of the scaffolds. Scaffold density provides information about the size, distribution and permeability of pores and the presence of structural defects in sintered ceramic frameworks [18]. Due to the hydrophobic properties of polymer, 96 % ethanol, which can pass easily through pores, was used instead of water. The mass of the ceramic sample (W) was measured, and a volume (V_1) of ethanol was poured into a graduated cylinder and measured. The sample was immersed in ethanol for 5 min until it became saturated (V_2). The discrepancy between

volumes ($V_1 - V_2$) represented the volume of the scaffold. The ethanol-soaked scaffold was removed from the graduated cylinder, and the remaining volume was recorded as V_3 . $V_1 - V_3$ represented the volume of ethanol absorbed by the scaffold [16].

The following equation calculates density of the scaffold (ρ) (Eq. 1).

$$\rho = \frac{W}{V_2 - V_3} \quad (1)$$

The following equation calculates the amount of open porosity of the scaffold (ε) (Eq. 2):

$$\varepsilon = \frac{V_1 - V_3}{V_2 - V_3} \quad (2)$$

2.6 Mechanical characterization

Machining and gripping the specimen is a major problem in the mechanical characterization of ceramic porous scaffolds: conventional methods of mechanical characterization, such as tensile, biaxial and impact tests are usually inapplicable to porous materials [18]. Compression impact tests for porous bone and NBG samples are instead used [16–19]. Compressive strength and compressive module tests for samples with and without P3HB coating were performed using a compression impact tester (SANTAM- Eng. Design Co. LTD.) with a 10-KN load cell based upon guidelines set in ASTM-D5024-95a. The dimensions of each sample were $20 \times 10 \times 10 \text{ mm}^3$ for the compression impact test. As ceramic scaffolds are fragile, the crosshead speed was set at 0.5 mm/min to prevent damage to the ceramic structure. The load carried by the sample was considered to be 30 % of the scaffold's original length. The elastic modulus was calculated as the slope of the initial linear portion of the stress–strain curve. The yield strength was determined from the cross point of the two tangents on the stress–strain curve around the yield point.

2.7 Bioactivity experiments in simulated body fluid (SBF)

The formation of a surface calcium phosphate (Ca–P) layer on the NBG/PHB scaffold was evaluated in SBF with solution ion concentrations similar to those of human blood plasma (Table 2) based on the formulation and method developed by Kokubo et al. [20]. The SBF solution was prepared by dissolving reagent-grade chemicals of NaCl, NaHCO_3 , KCl, $\text{K}_2\text{HPO}_4 \cdot 3\text{H}_2\text{O}$, $\text{MgCl}_2 \cdot 6\text{H}_2\text{O}$, $\text{CaCl}_2 \cdot 2\text{H}_2\text{O}$, Na_2SO_4 , and $(\text{CH}_2\text{OH})_3\text{CNH}_2$ in distilled water and buffered with 1-M HCl to a pH of 7.4 at 37 °C [20].

Disks measuring 10 mm in diameter were cut from the scaffolds. They were all immersed in SBF at 37 °C without vibration disturbance. The ratio between the sample and

solution volume was controlled to be 0.1. During the immersion period, the SBF was refreshed after 6 h of incubation followed by 24 and 48 h and then after every 3 days. The specimens were then collected after 1, 3, 7, 14 and 28 days of incubation. The immersed samples were removed from the SBF, washed with deionized water and dried in a vacuum drying oven. SEM (Philips XL30, The Netherlands) was used to study the surface morphology and microstructure. Energy dispersive X-ray analyzer (EDXA) directly connected to SEM was used to investigate, semi-quantitatively, the chemical composition of the mineral surface layer. For SEM test, the surface of each sample was coated with gold in advance, while for EDXA analysis, gold-coated technique was not applied for eliminating the effect of gold element. The solution chemical analyses were performed to determine changes of Ca ions as a function of the submersion time using a flame atomic absorption spectrophotometer. The pH of solution was measured at the end of immersion time periods to determine changes of pH as a function of the submersion time using a pH meter.

3 Results and discussion

3.1 NBG and ceramic scaffold

Figure 3a shows XRD spectra that the 45S5 NBG powder made at 1,400 °C within alumina plant during the 10-h mechanical alloying. It was noted that the obtained product was bioglass and no additional stable phase was found [21]. Then, by making solution and construction scaffolding at 600 °C, peak XRDs are shown in Fig. 3b, and the size of the crystals at 600 °C was obtained at 24–27 nm by Modified Scherrer equation (Monshi et al.), respectively [22]. Figure 3c shows the porous ceramic scaffold which at an angle of 32.575° at 1,000 °C, a peak is related to the apatite in this study it would be acted as an impurity along with bioglass. The results of XRD and FT-IR showed that the best temperature for construction of scaffolds is 600 °C, in which Na₂Ca₂Si₃O₉ crystal is obtained. The

resulting figure is accordance with the results of Chen et al. [17].

The results of XRF analysis of the powder sample produced using the melting method are presented in Table 1, which shows, with acceptable matching, that the weight percentages are similar to standard weight percentages of 45S5. These results confirm the production of bioglass with favorable weight percentages (45S5) [17].

The patterns of FT-IR bioactive glass 45S5 and bioactive glass ceramic scaffold are shown in Figs. 4a and b, respectively. A recent infrared analysis carried out by Boskey and Camacho [23] revealed that the main mineral components of bone are phosphate and carbonate which are related to hydroxyapatite and a series of absorption bands are related to the amide groups that are related to proteins (collagen) in the bone with absorption bands occurring in the range between 800 and 1,800 cm⁻¹ [23]. Comparison of the results related to the infrared spectrometer of bioactive glass 45S5 with scaffold heated at 600 °C shows that all the organic components of bone are removed after heating. For example, bands related to the amide groups which are carbonate impurities are usually found in small amounts in the bioactive glass structure. 1,395 and 1,453 cm⁻¹ band in the spectra of bioactive glass 45S5 are visible, but the spectra related to the heated scaffold were not observed. Evidence shows that heating bioactive glass scaffold leads to the removal of organic compounds; it also shows that polyurethane foam used in the preparation of scaffold during the heating process is completely out of the system.

Figure 5 shows that the particles mainly have semi-spherical morphology and the particle size is about 55–56 nm. Thus, the produced products can be considered for bone tissue engineering applications [24]. In order to prevent cracks in the ceramic structure, there should be sufficient time for burning of polymeric foams. Figure 6 shows the weight change of the polyurethane foam according to temperature. The figure shows that the main part of polymer was removed at temperatures between 230 and 600 °C; therefore, it is necessary to take into account the slow heating rate at this stage to prevent structural

Table 2 Comparison between porosity percentage, compressive strength and compressive modulus of NBG scaffold coated with and without P3HB

Sample	Mean porosity (%)	Compressive strength (MPa)	Compressive modulus (MPa)
S ₁	87	0.09 ± 0.02	1.47 ± 0.3
S ₂	82	0.3 ± 0.05	10.41 ± 0.5
S ₃	79.5	0.35 ± 0.05	14.05 ± 0.7

S₁ BG scaffold

S₂ BG scaffold coated by P3HB in 30 s

S₃ BG scaffold coated by P3HB in 1 min

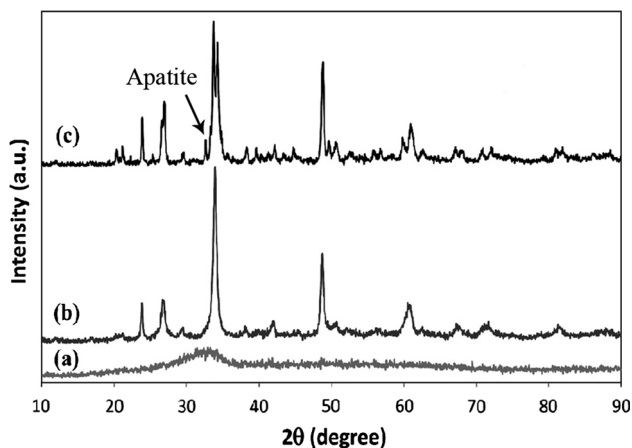


Fig. 3 Pattern of XRD analysis: *a* 45S5 NBG powder made at 1,400 °C, *b* bioglass scaffold at 600 °C and *c* bioglass scaffold at 1,000 °C

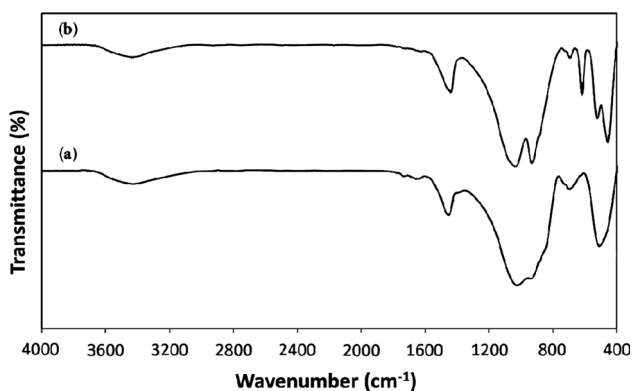


Fig. 4 Pattern of FT-IR analysis: *a* bioglass powder and *b* Porous ceramic scaffold of heat treatment at 600 °C

damage caused by emissions from thermal degradation of polymers. At temperatures above 600 °C, the polymer foam had a low weight decrease due to the amount of produced carbon from the decomposition of the polymer process dioxide. Complete combustion of polymeric foams occurred at 600 °C. Therefore, to prevent cracking and thermal shock, temperature increase with a heating rate of 2 °C/min reached 400 °C and then kept at this temperature for 1 h and again with a heating rate of 2 °C/min reached 600 °C and then for complete combustion of sponge, it was maintained for 6 h at the temperature mentioned above.

3.2 Bioglass scaffold with and without P3HB coating

Figure 7 shows the XRD pattern of the NBG scaffold with and without P3HB coating. In Fig. 7a, peaks related to the P3HB are evident, while the pattern in Fig. 7b indicates the process mentioned in Sects. 2–4 about the ceramic scaffold. Nanocomposite coating and the produced coated

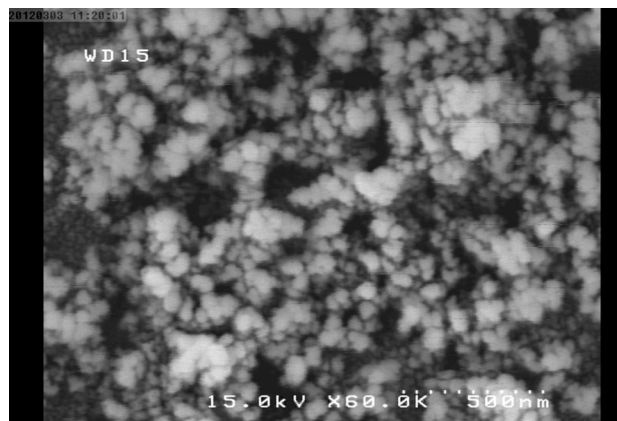


Fig. 5 FE-SEM of nano-bioglass powder

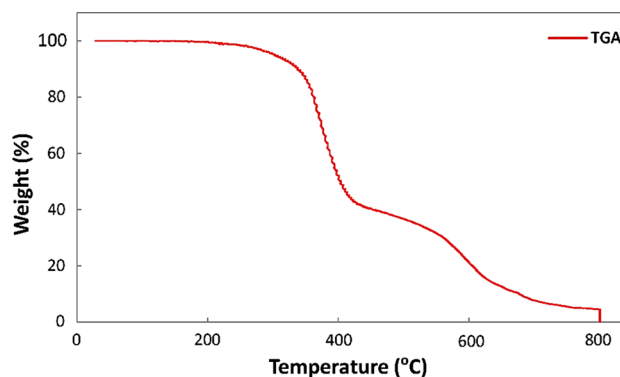


Fig. 6 Weight loss as a function of temperature (heating rate = 3 °C/min) for pyrolysis of polyurethane sponge

polymer scaffold data are shown in Fig. 7c. Based on comparisons with the standard JCPDS: 033-1161 scaffold after coating, the angle peaks of 14 and 17.13 indicate that the composite structure was indeed a nanocomposite scaffold.

Figure 8a shows FTIR diagram related to the P3HB, in which peaks of 1,126 and 1,172 cm⁻¹ are related to asymmetric and symmetric stretching vibrations of C–O bond, respectively. Groups CH₃ make sharp peaks due to the stretching vibration of this bond. P3HB has terminal hydroxyl groups that can be seen at the relevant peak within a range of 3,680–3,100 cm⁻¹. In the wavelength 1,720 cm⁻¹, a very sharp and clear peak was observed due to the stretching vibration of carbonyl groups. Absorption spectra of bioactive glass scaffold in Fig. 8b shows the peaks related to the presence of the main phase Na₂Ca₂Si₂O₆. As can be seen in Fig. 8c in the composite wavelength of 1,717 cm⁻¹, a short peak is composed of the carbonyl group which is related to carbonyl group of the spectra P3HB. Chart of P3HB in the wavelength 2,980 cm⁻¹, a peak is observed due to the stretching

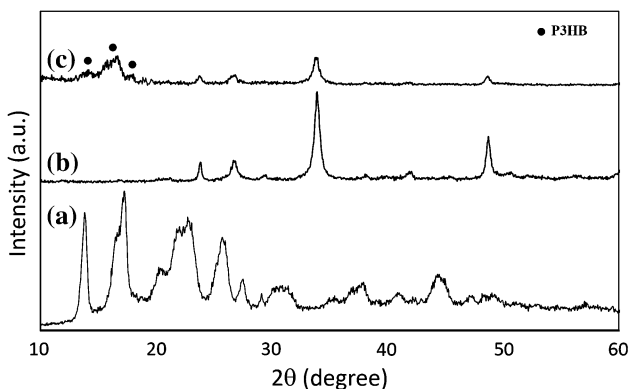


Fig. 7 Pattern of XRD analysis: (a) P3HB, (b) NBG-30 % scaffold and (c) NBG/P3HB composite scaffold according to standard of JCPDS:033-1161

vibration of C–H bond, the same peak in wavelength $2,981\text{ cm}^{-1}$ is visible in Fig. 8c.

For further evaluation of particle interactions NBG and P3HB, the FT-IR spectrum of this composite in comparison particles of NBG in two the absorption ranges $900\text{--}1,500\text{ cm}^{-1}$ and FT-IR composite spectra with pure polymer in the absorption range $1,600\text{--}3,000\text{ cm}^{-1}$ is shown more clearly in Fig. 9. As is evident, the peak absorption of carbonyl group P3HB in frequency $1,720\text{ cm}^{-1}$ is revealed sharper and clearer than the corresponding peak in the composite. In addition, this peak in the composite NBG/P3HB has been transferred to the lower wavelength of $1,717\text{ cm}^{-1}$. Carbonyl absorption peak shift to lower frequencies shows the potential occurrence of hydrogen bonds between the carbonyl groups in P3HB and hydroxyl groups and phosphate in NBG particles. In Fig. 9b, the graph of P3HB in the wavelength of $2,980\text{ cm}^{-1}$, a peak due to bond stretching vibration, is observed that is visible in the lower wavelength in NBG/P3HB composite. This phenomenon can support the distribution of polymer in the particles matrix NBG as smooth

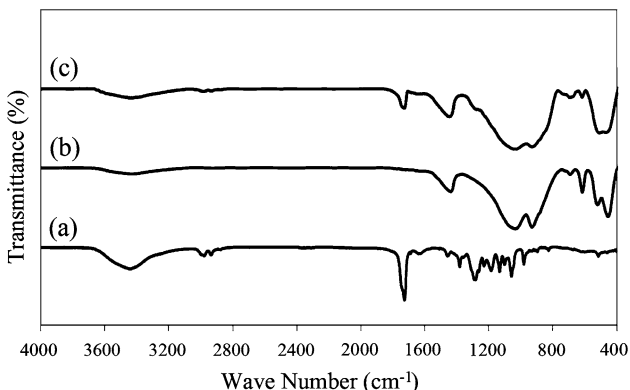


Fig. 8 Pattern of FT-IR analysis: a P3HB, b NBG-30 % scaffold and c NBG/P3HB composite scaffold

and efficient. Wavelengths of peaks in Fig. 9a have changed from $931, 1,035$ and $1,439\text{ cm}^{-1}$ in the bioactive glass scaffold to $931, 1,035$ and $1,449\text{ cm}^{-1}$ in the composite, respectively. This indicates the presence of bioactive glass particles in the composite structure.

As seen in Fig. 10, SEM images show uniform porosity in size between 200 and $600\text{ }\mu\text{m}$, which are suitable for immigration of osteoblasts [25]. Murphy et al. investigated the effect of pore size on cell adhesion, proliferation and migration in bone tissue engineering and found that scaffolds with pore size of $325\text{ }\mu\text{m}$ are suitable for bone tissue engineering [25]. Figure 10a shows the electron microscope images of polyurethane foam with open pores within a range of $300\text{--}700$ before immersion in the ceramic slurry. Figure 10b shows the porous ceramic scaffold with pore diameters ranging from 200 to $600\text{ }\mu\text{m}$. Figure 10c and d show the composite scaffold NBG/P3HB in two different magnifications. Based on SEM images and the results of the tests FT-IR and XRD, it is proved that it is a composite.

3.3 Compressive strength of scaffold with and without coating P3HB

The compressive strength test was performed on the samples with and without coating of the polymer, and the results are shown in Table 2. The results of compressive strength showed that compressive strength in uncoated polymer scaffolds was 0.09 Mpa , while the compressive strength in coated polymer scaffold was 0.35 Mpa . Table 2 also shows that with increasing immersion time of the polymer, the strength and modulus increase. In other

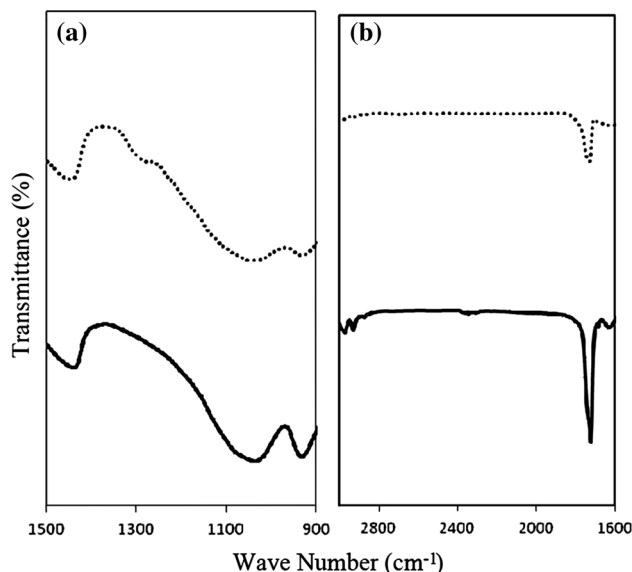


Fig. 9 Pattern of FT-IR analysis: a NBG and NBG/P3HB, b P3HB and NBG/P3HB

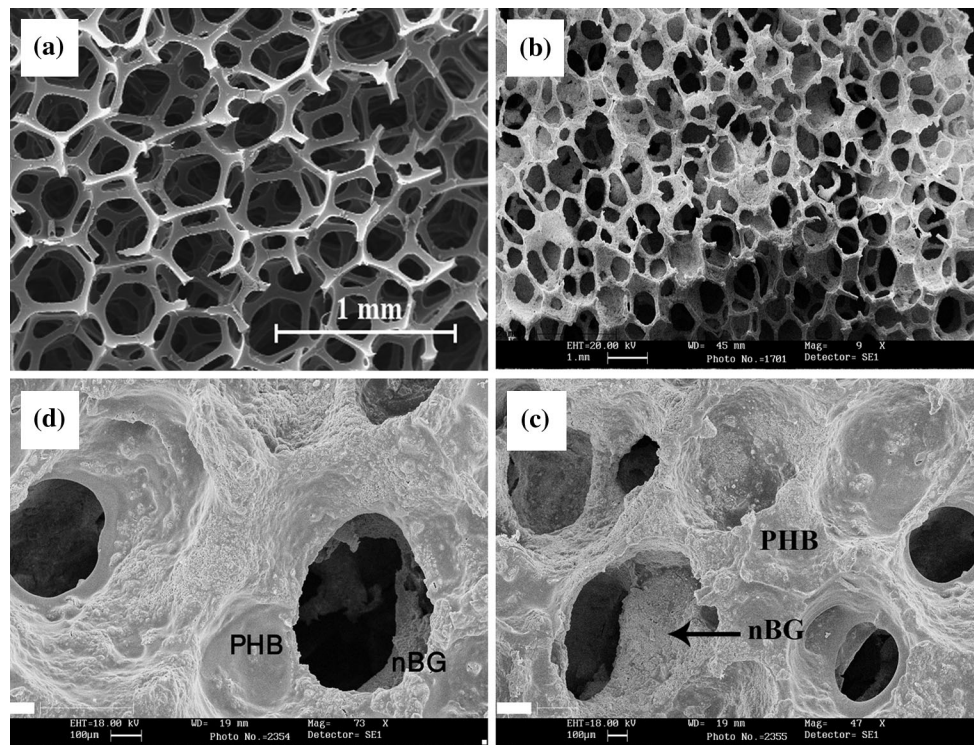


Fig. 10 **a** polyurethane sponge's image captured by SEM ($\times 50$), **b** cross section of NBG scaffold without polymer coating ($\times 50$), **c** cross section of NBG with P3HB coating ($\times 4,700$) and **d** cross section of NBG with P3HB coating at high magnification ($\times 7,300$)

studies, Callcut et al. [26] by polymeric sponge method with reinforced hydroxyapatite coating by glass is achieved with compressive strength between 0.01 and 0.175 MPa. Chen et al. [27] produced scaffolds from bioactive glass coated with a polymer PDLLA. The compressive strengths of the scaffold before and after coating were 0.045 and 0.3 MPa, respectively. Therefore, the fabricated scaffolds in this research have more compressive strength due to method of fabrication and presence of P3HB as a coated layer on bioglass scaffolds. Table 2 is also shows that by increasing the time of dipping in P3HB, the porosity is decreasing and the mechanical property is increasing which is because of more filling the pores with P3HB.

3.4 The study of bioactivity behavior of composite scaffolds

Based on the results of porosity percentage and compressive strength test results, the 30 wt% of porous bioglass scaffold with and without 1 min coating of 6 wt% of P3HB was selected as the optimally bioactive scaffolds.

To evaluate the bioactivity after placing the samples for 4 weeks in a solution of SBF, analysis of XRD, SEM and EDXA were carried out. Then, atomic absorption test was used to evaluate the absorption of calcium from the solution containing final SBF conducted on different days.

3.4.1 Thin film XRD test

To study the formation of hydroxyapatite on the surface of scaffolds an X-ray spectrometer with thin layer (XRD, PHILIPS PW 1390) was used with a growth rate 1° per minute, a voltage of 15 kV and a current of 30 mA; an analysis of radiation Cu $K\alpha$ and scattering angle 2θ of 30° – 40° due to the higher density of hydroxyapatite peaks in this region. Figure 11a is a peak related to natural hydroxyapatite [14]. Figure 11b shows the peaks of hydroxyapatite on the surface of uncoated scaffold; due to scaffolding Bioglass field, peaks of intensity are higher but Fig. 11c is related to the coating scaffold by P3HB during 1 min immersion; the intensity of these peaks decreases due to the presence of polymeric coating, and hydroxyapatite formation is minimal.

3.4.2 SEM and EDXA tests

3.4.2.1 Bioglass scaffold without coating with P3HB Figure 12 shows formation of hydroxyapatite on uncoated ceramic scaffolds for 7 and 28 days. Figure 12a is related to the formation of hydroxyapatite with a magnification of $\times 2,000$ on the 7th day; the maximum amount of the apatite formed on the surface of the scaffold. Figure 12b is related to the formation of hydroxyapatite with a

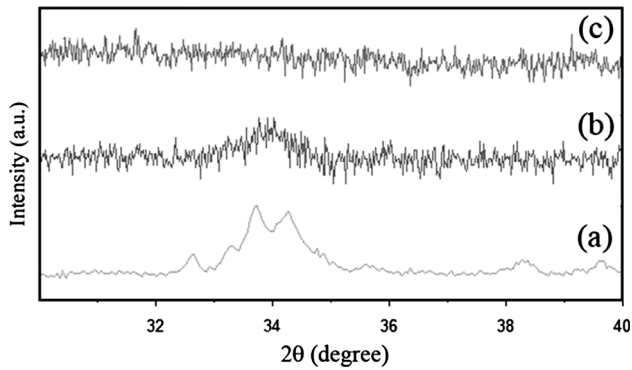


Fig. 11 a natural hydroxyapatite, b hydroxyapatite on the surface of without coated scaffold and c coating scaffold by P3HB during 1 min

magnification of $\times 2,000$ on the 28th day; the least apatite formed on the surface of the scaffold.

Figure 13 shows the results of EDXA of apatite produced on the surface of scaffold during the first week

(Fig. 13a) and the fourth weeks (Fig. 13b). It is observed that the formation of hydroxyapatite from SBF solution requires formation of an amorphous initial phase, which is the dehydrated amorphous tri-calcium phosphate capable of absorbing Ca^{2+} and PO_4^{2-} ions. It was observed that dehydrated di-calcium phosphate first forms sediment and then is hydrolyzed into hydroxyapatite from calcium [28].

3.4.2.2 Bioglass scaffold coated with P3HB Figure 14 shows the formation of hydroxyapatite on ceramic scaffold with coatings of P3HB at 7 and 28 days. Figure 14a is related to the formation of hydroxyapatite with a magnification of $\times 5,000$ on the 7th day, which is the lowest apatite formed on the surface of the scaffold. Figure 14b is related to the formation of hydroxyapatite with a magnification of $\times 5,000$ on 28th day, which is the maximum amount of the apatite formed on the surface of the scaffold.

Figure 15 shows the results of EDXA of apatite produced on the surface of scaffold during the first week

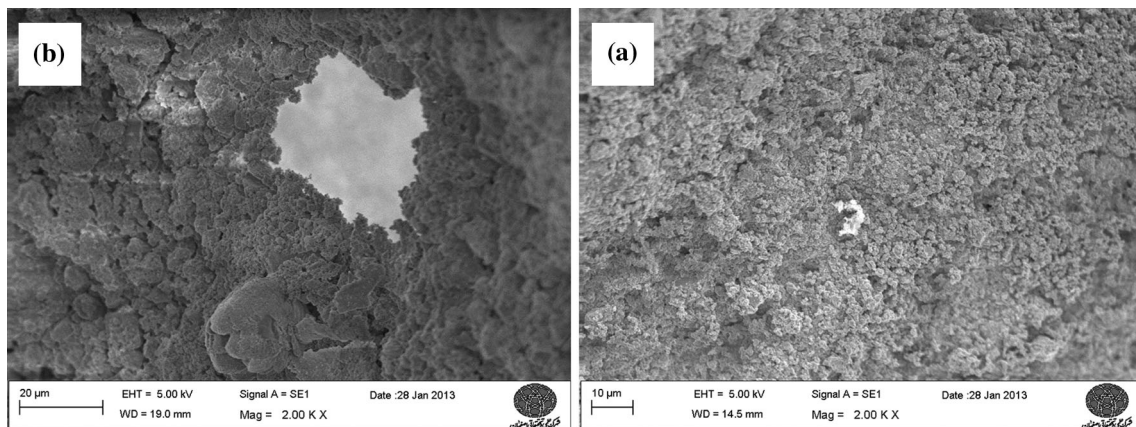


Fig. 12 SEM a magnification of $\times 2,000$ times 7th, b magnification of $\times 2,000$ times 28th

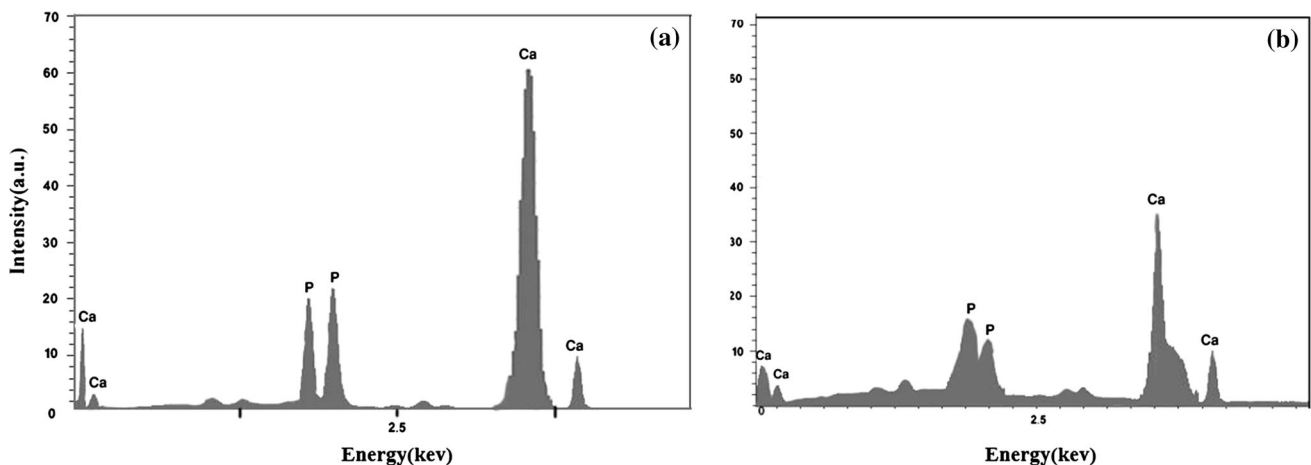


Fig. 13 EDXA a magnification of $\times 2,000$ times 7th, b magnification of $\times 2,000$ times 28th

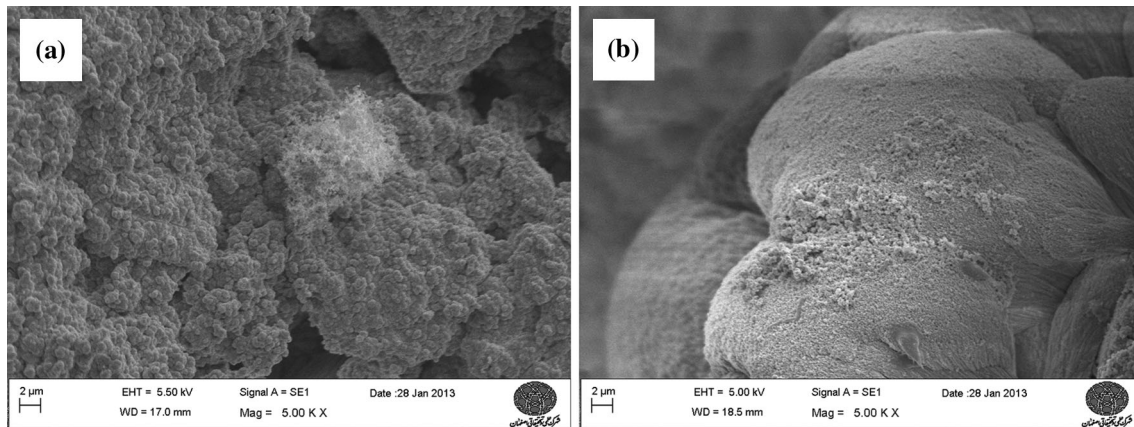


Fig. 14 SEM **a** magnification of $\times 5,000$ times 7th, **b** magnification of $\times 5,000$ times 28th

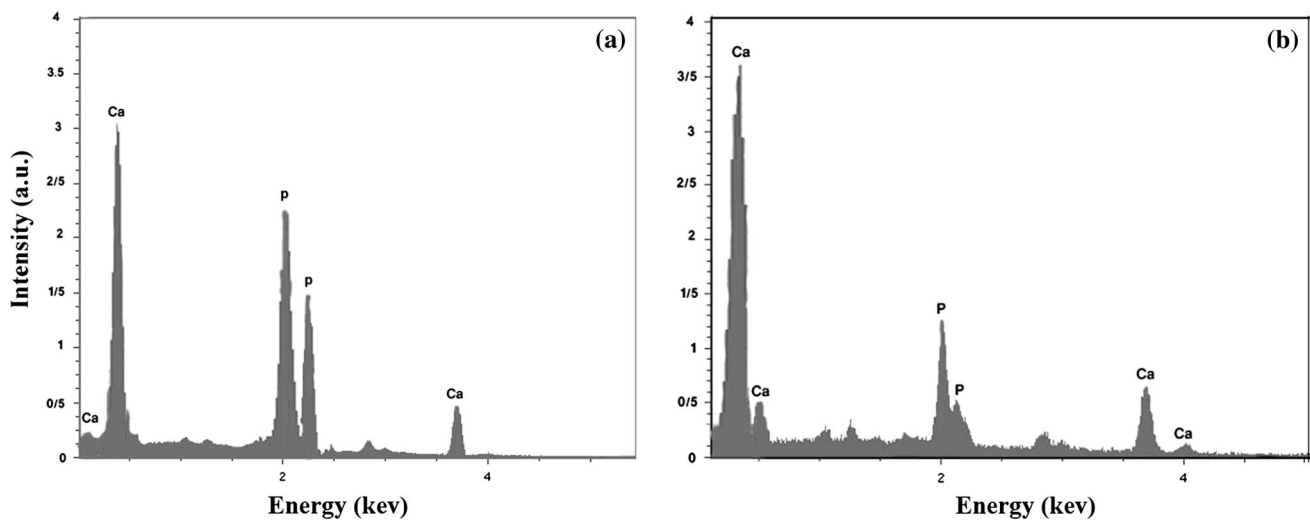


Fig. 15 EDXA **a** magnification of $\times 5,000$ times 7th, **b** magnification of $\times 5,000$ times 28th

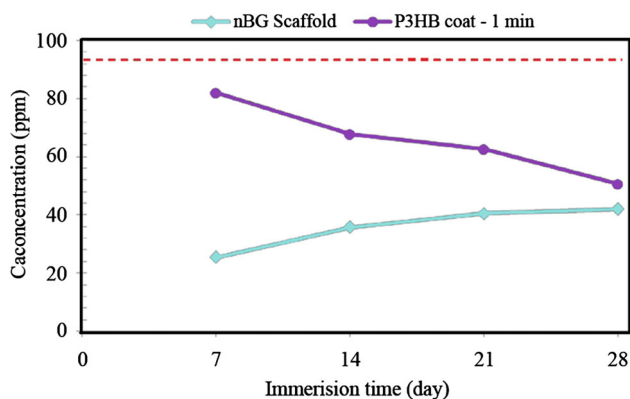


Fig. 16 Atomic absorption spectroscopy (AAS) analysis

(Fig. 15a) and the fourth week (Fig. 15b); which is the maximum amount of the apatite formed on the surface of the scaffold at the fourth week.

3.4.3 Atomic absorption spectroscopy (AAS) analysis

To investigate the amount of absorption of calcium atoms and their absorption percentage by scaffolding, an atomic absorption spectrometer was used (Fig. 16). The higher percentage of calcium atoms in solution indicates that the absorption was carried out by bioactive scaffolding and the scaffold was weaker in terms of bioactivity. It is appear in Fig. 16 that absorption of calcium ion on the bioglass scaffolds is opposite to that of the bioglass/P3HB scaffolds. It means that because of the coated surface of bioglass/P3HB scaffolds, apatite formation is increasing by time. A comparison of the bioactivity between nHA/P3HB [14] and our scaffolds showed that the atomic absorptions of the scaffolds were 70–89 and 25–82 ppm, respectively. In addition, based on higher stoichiometry of Ca/P in the nBG/P3HB scaffold and the thin-layer XRD results the higher bioactivity of nBG/P3HB scaffold compared to nHA/P3HB scaffold might be explained.

Therefore, the innovation of this research study compared to previous studies was the higher bioactivity of this scaffold.

4 Conclusions

In this study, the NBG ceramic scaffold was coated with P3HB polymer using polyurethane foam method. The results of FTIR, XRF and XRD analyses showed that the powder of bioactive NBG with particles sizes of 55–65 nm was produced as the background material. The results of XRD showed that according to the JCPDS 033-1161 standard, the scaffold was revealed after coating in angles 14° and 17.13° of peaks given that the standard is related to P3HB. It can be proved that the composite structure is a composite scaffold of NBG/P3HB with 0.09–0.35 MPa compressive strength and 80–87 % porosity. Bond absorption numbers in the test FTIR showed formation of the hydrogen bond between hydroxyl groups and Si–O bond of bioactive glass and carbonyl groups of P3HB and also it showed formation of composite scaffold. In addition, the results of XRD, EDXA, SEM and AAS analyses showed high bioactivity of the scaffold. Finally, given the results of porosity and mechanical and bioactive tests for tissue engineering, the best scaffold was the scaffold with 30 wt% of bioglass, with 6 wt% of P3HB.

References

- Hutmacher DW. Scaffolds in tissue engineering bone and cartilage. *Biomaterials*. 2000;21:2529–43.
- Gomes MA. Bone tissue engineering strategy based on starch scaffolds and bone marrow cells cultured in a flow perfusion bioreactor. PhD thesis. 2004;1:25–34.
- Lanza R, Langer R, Vacanti J. Principle of tissue engineering. 3rd ed. San Diego: Academic Press; 2007.
- Jeffrey O, Thomas A, Bruce A, Charles S. Bone tissue engineering. 4th ed. Boca Raton: CRC Press; 2005.
- Sehrooten J, Helsen JA. Adhesion of bioactive glass coating to Ti6Al4V oral implant. *Biomaterials*. 2000;21:46–191.
- Jones DA. Principles and prevention of corrosion. Singapore: MacMillan Publishing Company; 1992.
- Hajiali H, Karbasi S, Hosseinalipour M, Rezaie H. Effects of bioglass nanoparticles on bioactivity and mechanical property of poly(3hydroxybutyrate) scaffolds. *Scientia Iranica*. 2013;20:2306–13.
- Schüth F, Sing KSW, Weitkamp J. Handbook of porous solids: gelcasting foams for porous ceramics. Columbus: American Ceramic Society Bulletin; 2002. p. 2423–970.
- Akaraonye E, Keshavarz T, Roy I, Chem J. Production of poly-hydroxyalkanoates. *J Chem Technol Biotechnol*. 2010;85:732–43.
- Misra SK, et al. poly(3-hydroxybutyrate) multifunctional composite scaffolds for tissue engineering applications. *Biomaterials*. 2010;31:2806–15.
- Li W, Laurencin C, Catterson E, Tuan R, Ko F. Electrospun nanofibrous structure: a novel scaffold for tissue engineering. *J Biomed Mater Res*. 2002;60:613–21.
- Knowles JC, Hastings GW. Development of a degradable composite for orthopaedic use. *Biomaterials*. 1992;13:491–6.
- Bretcanu O, et al. Biodegradable polymer coated 45S5 Bioglass-derived glass-ceramic scaffolds for bone tissue engineering. *Eur J Glass Sci Technol*. 2007;48:227–34.
- Foroughi M, Karbasi S, Ebrahimi-Kahrizangi R. Physical and mechanical properties of a poly-3-hydroxybutyrate coated nanocrystalline hydroxyapatite scaffold for bone tissue engineering. *J Porous Mater*. 2012;19:667–75.
- Saadat A, Behnamghader AA, Karbasi S, Abedi D, Soleimani M, Shafiee A. Comparison of acellular and cellular bioactivity of poly 3-hydroxybutyrate/hydroxyapatite nanocomposite and poly 3-hydroxybutyrate scaffolds. *J Biotechnol Bioprocess Eng*. 2013; 18:587–93.
- Ramay H, Zhang M. Preparation of porous hydroxyapatite scaffolds by combination of the gel-casting and polymer sponge methods. *Biomaterials*. 2003;24:3293–302.
- Chen QZ, Thompson ID, Boccaccini AR. 45S5 bioglass-derived glass ceramic scaffolds for bone tissue engineering. *Biomaterials*. 2006;27:2414–25.
- Hodgskinson R, Currey JD. Effect of variation in structure on Young's modulus of cancellous bone. *J Eng Med*. 1986;204:115–21.
- Hing KA, Best SM, Bonfield W. Characterization of porous-hydroxyapatite. *J Mater Sci*. 1999;10:135–45.
- Kokubo T, Takadama H. How useful is SBF in predicting in vivo bone bioactivity? *Biomaterials*. 2006;27:2907–15.
- Hench LL. The story of bioglass. *J Mater Sci*. 2006;17:967–78.
- Monshi A, Foroughi MR, Monshi MR. Modified Scherrer equation to estimate more accurately nano-crystallite size using XRD. *World J Nano Sci Eng*. 2012;2:154–60.
- Boskey A, Camacho N. FT-IR imaging of native and tissue engineered bone and cartilage. *Biomaterials*. 2006;28:2465–78.
- Zin-Kook K, Jeong-Jung O, Hisamichi K. Architecture of porous hydroxyapatite scaffolds using polymer foam process. *J Biomech Sci Eng*. 2009;4:377–83.
- Murphy CM, Brien MG. The effect of mean pore size on cell attachment proliferation and migration in collagen glycosaminoglycan scaffolds for bone tissue engineering. *Biomaterials*. 2010;31:461–6.
- Callcut S, Knowles JC. Correlation between structure and compressive strength in a reticulate glass-reinforced hydroxyapatite foam. *J Mater Sci Mater Med*. 2002;13:485–9.
- Chen QZ, Boccaccini AR. Poly(DL-lactide) coated 45S5 bioglass-based scaffolds: processing and characterisation. *J Biomed Mater Res*. 2006;77:445–52.
- Landi E, Tampieri A, Celotti G, Sprio S. Densification behaviour and mechanisms of synthetic hydroxyapatites. *J Eur Ceram Soc*. 2000;20:2377–87.